Available online at www.sciencedirect.com

ScienceDirect

Advances in Space Research 55 (2015) 2414–2426

ADVANCES IN SPACE RESEARCH (a COSPAR publication)

www.elsevier.com/locate/asr

Mars methane analogue mission: Mission simulation and rover operations at Jeffrey Mine and Norbestos Mine Quebec, Canada

A. Qadi [a,*], E. Cloutis [b], C. Samson [c], L. Whyte [d], A. Ellery [e], J.F. Bell III [f], G. Berard [b], A. Boivin [c], E. Haddad [g], J. Lavoie [g], W. Jamroz [g], R. Kruzelecky [g], A. Mack [e], P. Mann [b], K. Olsen [h], M. Perrot [i], D. Popa [d], T. Rhind [b], R. Sharma [b], J. Stromberg [b], K. Strong [h], A. Tremblay [i], R. Wilhelm [d], B. Wing [j], B. Wong [g]

[a] Dept. of Mechanical and Transportation Technology, Algonquin College, Ottawa, ON K2G 1V8, Canada
[b] Dept. of Geography, 515 Portage Ave., University of Winnipeg, Winnipeg, MB R3B 2E9, Canada
[c] Dept. of Earth Sciences, Carleton University, Ottawa, ON K1S 5B6, Canada
[d] Dept. of Natural Resources, McGill University, Ste. Anne de Bellevue, QC H9X 3V9, Canada
[e] Dept. of Mechanical & Aerospace Engineering, Carleton University, Ottawa, ON K1S 5B6, Canada
[f] School of Earth & Space Exploration, Arizona State University, Box 871404, Tempe, AZ 85287-1404, USA
[g] MPB Communications Inc., Pointe-Claire, QC H9R 1E9, Canada
[h] Dept. of Physics, University of Toronto, Toronto, ON M5S 1A7, Canada
[i] Département des Sciences de la Terre et de l'Atmosphère, Université du Québec à Montréal, Montreal, QC H3C 3P8, Canada
[j] Dept. of Earth & Planetary Sciences, McGill University, Montreal, QC H3A 2A7, Canada

Received 19 September 2012; received in revised form 17 November 2014; accepted 7 December 2014
Available online 15 December 2014

Abstract

The Canadian Space Agency (CSA), through its Analogue Missions program, supported a microrover-based analogue mission designed to simulate a Mars rover mission geared toward identifying and characterizing methane emissions on Mars. The analogue mission included two, progressively more complex, deployments in open-pit asbestos mines where methane can be generated from the weathering of olivine into serpentine: the Jeffrey mine deployment (June 2011) and the Norbestos mine deployment (June 2012). At the Jeffrey Mine, testing was conducted over 4 days using a modified off-the-shelf Pioneer rover and scientific instruments including Raman spectrometer, Picarro methane detector, hyperspectral point spectrometer and electromagnetic induction sounder for testing rock and gas samples. At the Norbestos Mine, we used the research Kapvik microrover which features enhanced autonomous navigation capabilities and a wider array of scientific instruments. This paper describes the rover operations in terms of planning, deployment, communication and equipment setup, rover path parameters and instrument performance. Overall, the deployments suggest that a search strategy of "follow the methane" is not practical given the mechanisms of methane dispersion. Rather, identification of features related to methane sources based on image tone/color and texture from panoramic imagery is more profitable.

Keywords: Mars methane emissions; Planetary exploration microrover; Rover operations; Autonomous science; Analogue mission; Asbestos mine

1. Introduction, goals and approach

The search for signs of past or extant life on Mars is a high priority for future Mars exploration (e.g. MEPAG (2010)). This search will likely be undertaken with a variety of landed and orbital missions. The Canadian Space Agency (CSA), through its Analogue Missions program, supported a microrover-based analogue mission designed to simulate a Mars rover mission geared towards identifying and characterizing methane emissions on Mars. The

* Corresponding author.
E-mail address: qadia@algonquincollege.com (A. Qadi).

http://dx.doi.org/10.1016/j.asr.2014.12.008
0273-1177/

overall Mars methane analogue mission included the following activities (listed in chronological order): site evaluation visits leading to the selection of Jeffrey Mine (June 2010, November 2011) (Boivin et al., 2011; Cloutis et al., 2011b), major deployment at Jeffrey mine (13–16 June 2011) (Boivin et al., 2012, 2013; Cloutis et al., 2012), complementary imaging survey at Jeffrey Mine (3–4 October 2011) (Boivin et al., 2013), site evaluation visits leading to the selection of Norbestos Mine (November 2011 and May 2012), and major deployment at Norbestos (18–22 June 2012) (Cloutis et al., 2013; Ralchenko et al., 2013). This paper focuses on the two major deployments at the Jeffrey and Norbestos mines.

The Mars Methane Mission encompasses a wide range of operational, technical and scientific goals:

1. (Operational goal) Develop mission planning and operational methodologies to accomplish science remotely from a microrover platform based on simulated Mars-like communications links and data capacities.
2. (Operational goal) Acquire mission operational experience for remote operations in realistic simulated conditions.
3. (Technical goal) Select and validate the instrumentation required to detect the presence of methane in support of planetary geological and astrobiological investigations.
4. (Scientific goal) Study the correlation between methane emissions and the local geology – especially the presence of serpentine deposits and hydrated minerals, emission pathways, and associated microbiological activity.
5. (Overarching goal) Provide recommendations on the scientific, operational and technical advancement required to support future microrover-based Mars missions.

The analogue mission was based on the notion that enhanced methane concentrations on the surface will be correlated with structural elements such as joints and faults. This correlation assumes that methane production is greater at depth than in the surface, and that these structural elements provide enhanced pathways for methane release to the atmosphere. The deployments included a combination of microrover-mounted instruments and handheld units, supplemented by sample (gas, rock) collection in the field for off-line analysis and laboratory verification of field results.

2. Methane detection and site selection

The recent discovery of methane in the Mars atmosphere (Mumma et al., 2003, 2009; Formisano et al., 2004; Krasnopolsky et al., 2004), is one of the key drivers for this analogue mission. While both the mechanism of formation and regional source of this methane are currently poorly constrained, one scenario was that the methane is being processed as a byproduct of weathering of serpentinites. It should be noted that this discovery is not without controversy (e.g. Zahnle et al. (2011)). This is a process that operates on Earth and can proceed both biogenically and abiogenically (Klein and Bach, 2009; McCollom and Seewald, 2001). Low-temperature abiogenic methane generation in terrestrial environments is now well-documented (e.g. Etiope and Sherwood Lollar (2013), Etiope et al. (2013), Etiope and Schoell (2014), and references therein). Briefly in this scenario, abiogenic methane can be generated via weathering of preexisting olivines to serpentine and magnesium carbonates through interactions with CO_2-charged water (Barnes et al., 1978). Biogenic methane can be produced in serpentinized terrains by methanogenic microorganisms via chemosynthesis (e.g. Schulte et al. (2006), Lang et al. (2012)). While the precise locations on Mars where this methane is being generated are unknown, there does appear to be a possible correlation between elevated methane concentrations in the Mars atmosphere and phyllosilicate-bearing regions (Mumma et al., 2009). This correlation was the primary driver for deciding to conduct the microrover analogue mission in a representative terrestrial serpentinized environment.

Our search for a suitable analogue site focused on the Appalachian ophiolites in Southern Quebec (Hebert and Laurent, 1989; Normand and Williams-Jones, 2007; Schroetter et al., 2005; Tremblay and Castonguay, 2002; Barnes et al., 1978; Klein and Bach, 2009; McCollom and Seewald, 2001). Whether methane production in serpentinite deposits in this region is actively proceeding is not well constrained, but there is strong evidence of methane production in the past (Normand and Williams-Jones, 2007). This region was chosen because of the expectation that methane is being produced in serpentinized terrains (albeit at low levels), and because putative detections of methane on Mars coincide with areas that have surficial serpentine (Ehlmann et al., 2008). This region contains a large number of active and abandoned open-pit mines, providing a wide range of terrain types for microrover trials. One of the project requirements stipulated by the CSA was to test the microrover over traverse distances of up to 500 m. This limited the suitability of some potential analogue sites that we had identified in the region.

Investigation of possible sites was conducted in 2010 and the team selected the Jeffrey Mine in Asbestos, Quebec, for the first deployment based on a number of criteria including suitable geology, probable subsurface methane generation, safety, accessibility and trafficability (Boivin et al., 2011; Cloutis et al., 2011a,b).

In the site selection process, the Norbestos Mine ranked as highly as the Jeffrey Mine, but at the time access to Norbestos was not known. The Norbestos mine also possessed several advantages over the Jeffrey mine that included: (1) a wider range of weathered lithologies; (2) a greater variety of surface types and slopes (which could be used to better assess rover performance on diverse terrains); (3) no restrictions on the number of hours the team could spend at the site; (4) easy road access; and (5) good communication lines of sight. When access to the Jeffrey Mine became

uncertain for 2012, the Norbestos mine was selected for the second deployment.

Pre-deployment visits to the Norbestos site were conducted in November 2011 and May 2012. Trafficability was assessed and ground-level gas samples were acquired to determine whether elevated methane levels were present at the site. These site visits helped to determine that slightly elevated methane was present at some portions of the site, and suitable areas for the rover deployment were available. The site visits also served to identify locations for the communications relays between the rover, base station, and operations centre.

3. Jeffrey Mine Deployment

3.1. Experimental setup and approach

The Jeffrey mine, located at 45 47′N 71 56′W at the edge of the town of Asbestos, Quebec, is one of the largest open-pit asbestos mines in the world. The mine includes a 700 m deep open pit in addition to an underground mine. All the experiments of the Mars methane analogue mission were carried out in the open pit (Fig. 1).

The Jeffrey mine deployment was designed to:

1. Control the rover from a remote location and test different path lengths and way point differences.
2. Search directly for methane emissions and track them to their source.
3. Identify tectonic features suitable for the release of subsurface methane (joint, fractures, fissures).
4. Map site geology to assess relationships between methane release and "suitable" mineralogy (i.e. serpentine and magnesium-carbonate).

The rover used was a Pioneer 3-AT (Pioneer, 2007) equipped with one mounted vision camera and RF communication to a remote control station (Fig. 2). The vision camera was mounted on the rover using a rigid platform with zero degrees of freedom.

The instrument suite included: an ASD point spectrometer (0.35–2.5 μm); a Raman point spectrometer (100–2200 cm^{-1}); a Picarro methane detector; a color imager; and an electromagnetic induction sounder (EMIS) (Boivin et al., 2012, 2013) (Fig. 3). These instruments have not yet been miniaturized and therefore could not be directly mounted on the rover (Table 1).

A communications (VPN) station was established close to the top of the mine to enable communications between the field team, the science team located in Pointe Claire, QC, and the operations team located at CSA headquarters in Saint-Hubert, QC (Fig. 4). This architecture simulates robotic operations on Mars commanded from a base on Earth (Fig. 5). The setup also included a base station

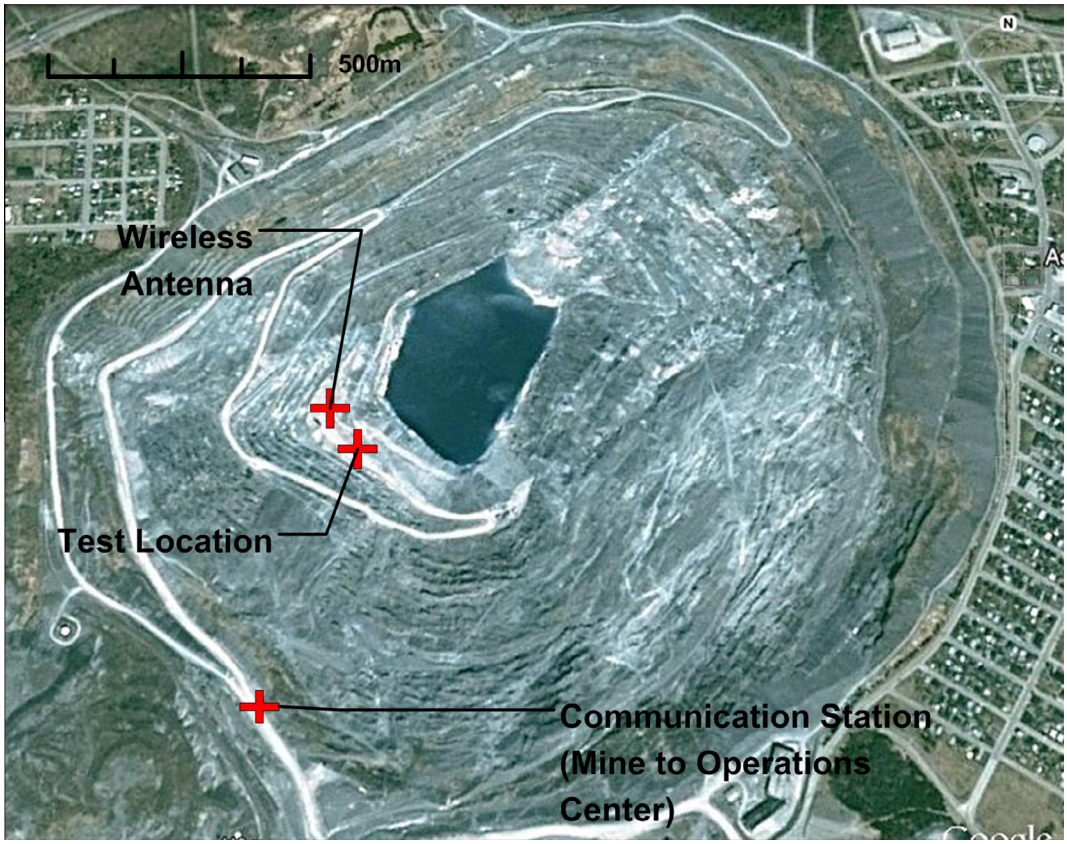

Fig. 1. Satellite view of the Jeffrey mine, Quebec from Google Earth.

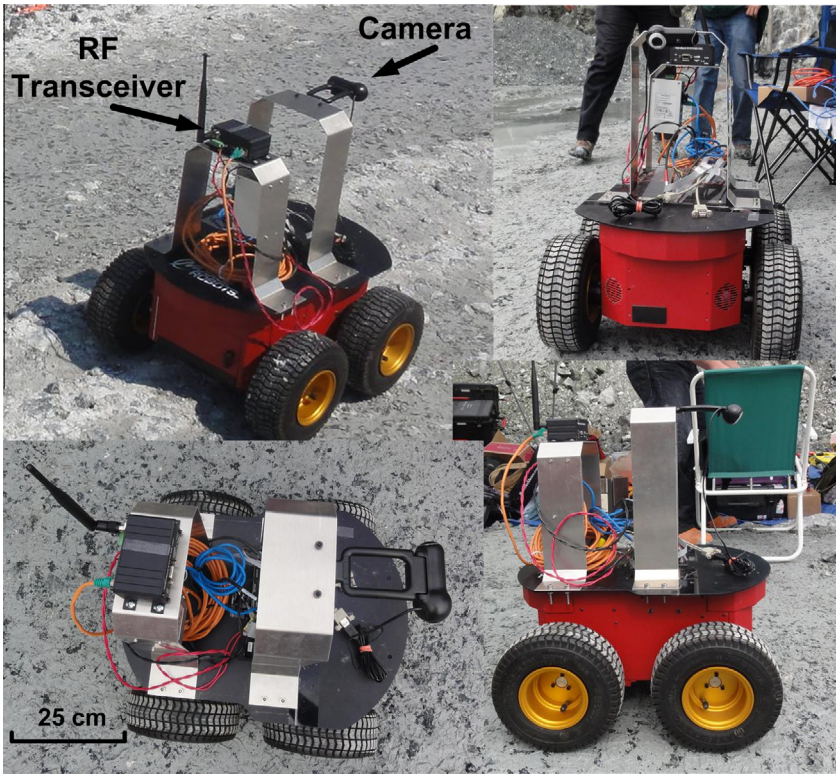

Fig. 2. Pioneer rover.

Fig. 3. EMIS mounted on a fiberglass with Pioneer rover in the background (mine test site).

equipped with a laptop computer and RF link to control the Pioneer rover and upload data (Fig. 6).

3.2. Operations

Long and short rover traverses were conducted during three days in the field. In all cases, the experiments were carried out in the following order:

1. Send command to rover from base station to move one step.
2. Send command from base station to rover to turn left (towards mine wall) and acquire an image.
3. Send command from base station to rover to turn right, orientation straight (towards path) then acquire a second image.
4. Send command from the base station to rover to turn right (away from mine wall) then acquire a third image.
5. The location where the rover has stopped was marked with a plastic cone and a paint mark representing the distance along the path.
6. The following actions were taken at the marked spot:
   (a) A rock sample was retrieved and brought back to the base station and examined by both Raman and ASD.
   (b) A gas sample was retrieved from and brought back to the Picarro for analysis.

After the rover traversed the path, the EMIS was moved along the same path acquiring electrical conductivity and magnetic susceptibility data to characterize the local

Table 1
Instruments used for the Mars methane analogue mission. Core instruments were essential to achieve the science goals of the mission; non-core instruments were demonstrated as they might prove useful in future deployments.

Instrument	Capability	Jeffrey mine	Norbestos mine	Mounted on rover	Core instrument
Rover Pioneer 3-AT	Mobility	√		N/A	N/A
Rover Kapvik	Mobility		√	N/A	N/A
Raman point spectrometer B&Wtek 532 nm	Raman emission features	√	√		√
Hyperspectral point spectrometer ASD FieldSpec Pro HR	Reflectance spectra	√	√		√
UV-induced fluorescence spectrometer	Fluorescence emission features		√		√
Picarro G2132 methane detector	Methane detection and C isotopic analysis by infrared transmission	√	√		√
Visible hyperspectral imager	Reflectance spectral images		√		
Electromagnetic induction sounder Dualem-2	Measurement of electrical conductivity and magnetic susceptibility at depth <3 m	√	√		
Stereo three-color cameras (Bumblebee-3)	Acquisition of stereo images	√	√	√	√
Three-band UV–vis imager	Acquisition of UV images		√	√	

Fig. 4. Wireless network antenna at the Jeffery mine. Its location is indicated in Fig. 1.

geology and especially identify joints and faults (Boivin et al., 2012, 2013).

Long traverse goal: Traverse 100 m with 5 m increments (a length of 100 m was the maximum that the site could physically accommodate; allocated time: day 1 of the deployment). The starting point was 8 m away from the base station. Table 2 shows the actual distances traveled by the rover: the distances were measured by using markers at robot stoppage points after each step. Accomplished Distance: 45.30 m in 5 m increments. This was the maximum that could be accomplished in the allocated time.

Table 2
Long traverse path at the Jeffrey mine test site. A rock sample and a gas sample were retrieved at each stoppage point.

Stoppage point	Distance traveled (m)
0	0
1	4.95
2	9.95
3	15.30
4	20.30
5	25.25
6	30.05
7	35.70
8	41.30
9	45.20

Short traverse goal: Traverse with 1 meter increments (allocated time: days 2–3 of the deployment). The short traverse location started from the same point as Test 1 (Fig. 7). However, due to communication problems, only 6 readings of one meter spacing were accomplished. The problem was due to the loss of line of sight between the station and the rover. This problem was solved by changing the site of the base station so that a clear line of sight was established with the rover. From this new location, two more short traverses were accomplished with a total distance traveled of 10.25 and 24.30 m.

3.3. Discussion

The utility of the various science instruments was assessed as part of the deployment. It was found that, at least for this terrain, the reflectance and Raman spectrometers provided largely similar data on mineralogy/geology (Figs. 8 and 9). Both instruments could identify the presence of the major mineral phases at the site: olivine, serpentinite, and iron oxides (hematite). In the reflectance spectra (Fig. 8), the presence of olivine is most recognizable

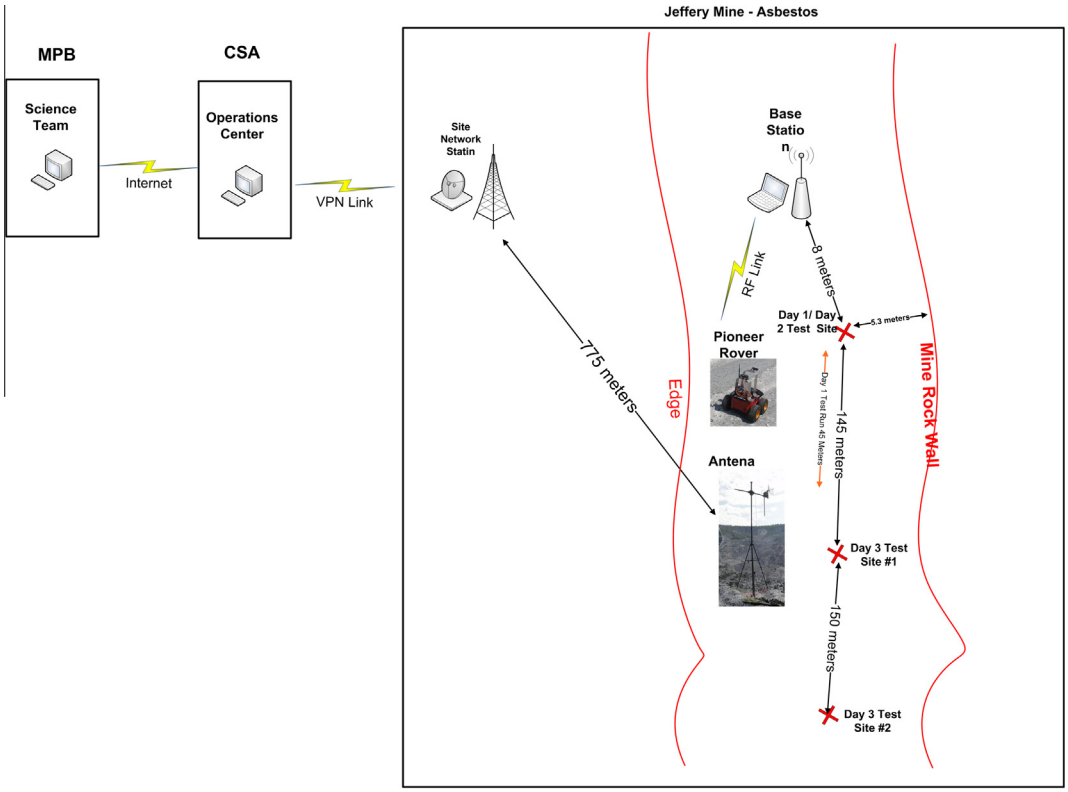

Fig. 5. Test location set up configuration.

Fig. 6. Base station set up showing Pioneer rover and Picarro sensor at the Jeffrey mine test site.

Fig. 7. Short traverse 1 (Jeffrey mine).

by the broad absorption band near 1.05 microns due to ferrous iron crystal field transitions, which is most evident in the least-altered ASD1.002 spectrum. Serpentine is most recognizable by the set of narrow absorption bands near 2.32 microns due to Mg-OH combination bands. It is also identified on the basis of the narrowness and wavelength position of the OH band near 1.4 microns, although this feature is less specific to serpentinite. Iron oxides (hematite) is most evident from the steep reflectance dropoff of ~0.6 microns due to ferric iron-oxygen charge transfers (e.g. Clark et al. (1990), Burns (1993)). For the Raman spectrum (Fig. 9), the presence of serpentine is most recognizable by the Raman peaks near 200, 390 and 700 cm^{-1}. Hematite is identified by the Raman peak that appears as a shoulder near 430 cm^{-1} and broader peak near 1400 cm^{-1}. Olivine is expected to exhibit its strongest Raman peak in the 800–900 cm^{-1} region, but these are not evident in the presented spectrum because it has been extensively altered to serpentine (peak identifications based on the RRUFF database: http://rruff.info). The methane analyzer was able to

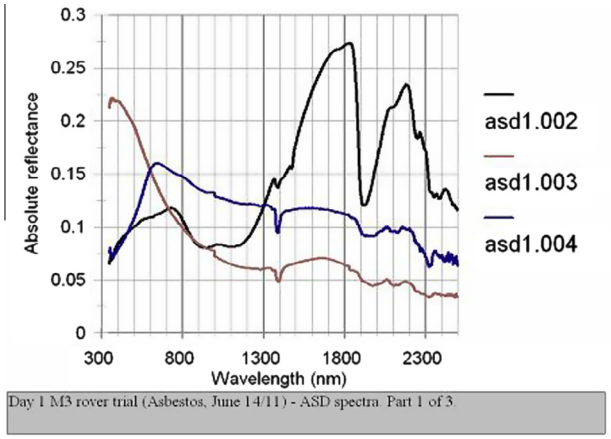

Fig. 8. Reflectance spectra of serpentinite from site (Jeffrey mine).

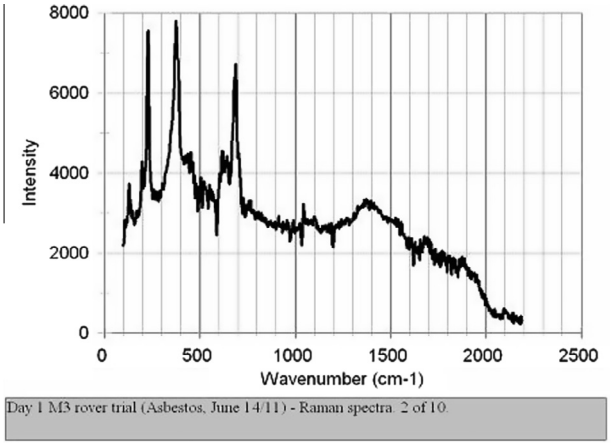

Fig. 9. Raman spectrum of an oxidized serpentinite from the Jeffrey mine rover traverse.

provide rapid analysis (~5–6 min) of the methane concentrations as well as 13C/12C ratios for sites where methane was present above the detection limit (−20 ppm). DNA recovered from the methane source (borehole) proved to originate from methanogenic Archaea demonstrating biological source. Yet, the delta C13/C12 ranged from ~−31% to −36%, which is elevated in 13C above measurements generally reported for methane directly produced from methanogenesis (>~−60–−70%). This suggested a mixed source of methane, both biogenic and abiogenic, which is significant as the site is not located in an area of hydrothermal activity. The EMIS was well-suited for identifying major near-surface (approximately 2 meters depth) discontinuities, indicative of subsurface fractures and changes in lithology (Boivin et al., 2012, 2013).

The major findings from this deployment, some of which influenced the 2012 deployment, were (Cloutis et al., 2012):

1. Tone in the color imagery was used to identify features that were felt to be of interest for target identification: specifically, searching the imagery for iron oxide staining and wetness; the former being possibly indicative of previous subsurface seepage and the latter indicative of present subsurface seepage. This focus was based on the expectation that signs of seepage could correlate with pathways for the release of subsurface generated methane. Textural analysis of the color imagery was focused on identifying surface cracks, joints or fissures, which would also be indicative of possible pathways for release of subsurface methane.
2. It appears that methane can be produced abiogenically in serpentinized terrains located away from heat sources;
3. Following methane gradients to a source is likely not viable, as methane was found to decrease to background rates within ~1 m horizontally from its point source. These detection limits are obviously a factor of the particular instrument used, and must also be considered in light of measurements uncertainties inherent in the instrument and the natural variability of methane in the atmosphere. Given that methane dissipates rapidly, detection of methane point sources would only be feasible in close proximity to a source (Olsen et al., 2012). Therefore, a more profitable approach would be to identify targets (either from orbit or on the surface) that may be associated with methane release. In the case of Mars, focusing on phyllosilicate-rich regions may improve targeting as such areas appear to correlate with the elevated methane levels putatively detected in the Martian atmosphere.
4. Deployment of the electromagnetic induction sounder (EMIS), towed along the ground, showed that EMIS was capable of clearly discriminating the shear zone that defines the contact between the serpentinite ore body and adjacent slate unit (Boivin et al., 2012, 2013).

4. Norbestos Mine Deployment

4.1. Experimental setup and approach

Lessons learned at the Jeffrey mine were instrumental in informing the sequence of operations at Norbestos. These included:

- The fact that methane concentrations falls rapidly (within 1 meter) to background levels from methane point sources. This was confirmed in open air tests conducted in May 2012 and modeling (Olsen et al., 2012).
- Conduits from the subsurface are high-priority targets for methane measurements, as they provide release paths for subsurface-generated methane. Targets of interest of this type include cracks and fissures. It these features also show evidence of color differences with the surroundings (such as iron staining) or water staining, they are of even higher priority.

At the Norbestos Mine (Fig. 10), target selection was based on the following sequence of events (Fig. 11):

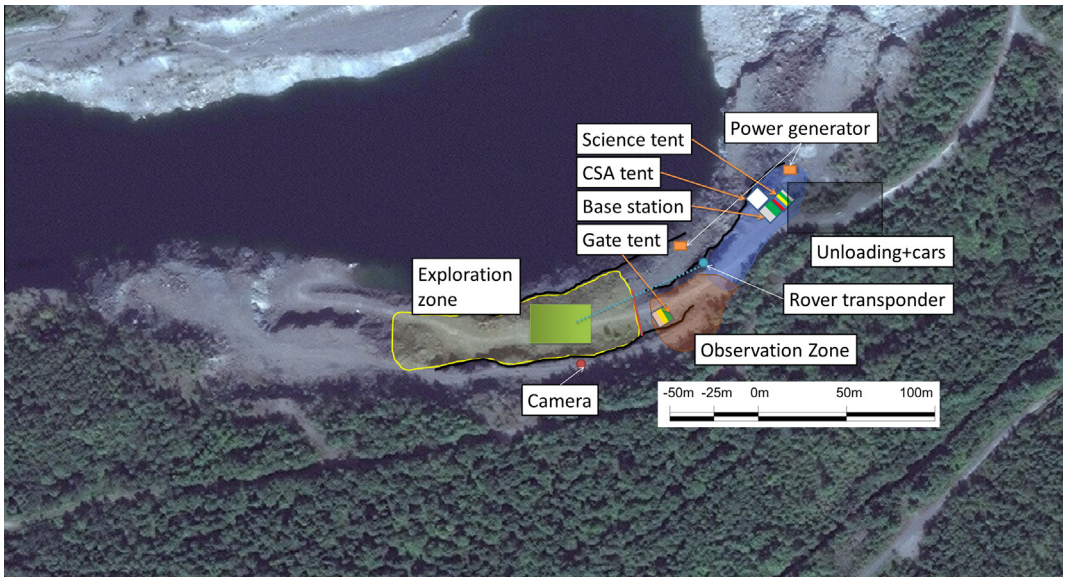

Fig. 10. Aerial view of the Norbestos test site. Targets were located in the green area (Fig. 13). Imagery source: Bing. (For interpretation of the references to color in this figure legend, the reader is referred to the web version of this article.)

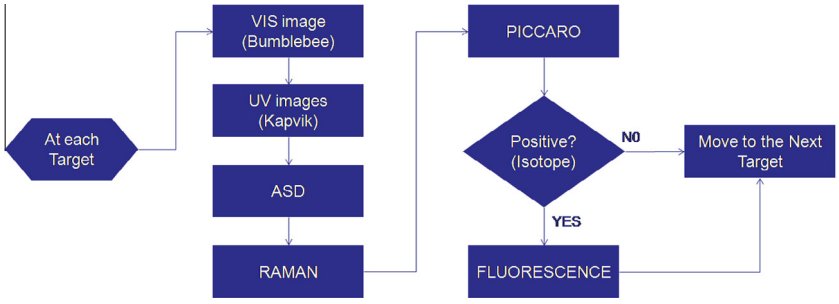

Fig. 11. Flowchart of measurements at a selected target (Norbestos mine).

1. Acquire a panoramic multispectral image of the surrounding area to a distance greater or equal to 10 m for path selection and area scouting; conduct measurements of ambient atmospheric methane concentration showing variations with distance from the source. These two activities are requirements stipulated by the CSA.
2. Analyze panchromatic imagery to identify the presence of structural elements (e.g. faults, joints, fractures) that form the first level of targets of interest.
3. Analyze multispectral imagery (by science team at science operations center) to determine whether color differences exist in the scene that may be indicative of changes in lithology that could be significant.
4. Select and rank targets of interest and pass on selections to navigation team to determine accessibility.

Once a target was selected, measurements included acquisition of multispectral images, UV–vis images, and hyperspectral reflectance and Raman spectra, and methane measurements at 0, 12, and 24 cm from the target of interest. If methane concentrations are enhanced, also conduct UV fluorescence imaging of the target (with an excitation wavelength of 405 nm), ideally below ground level, to determine the presence of any UV-fluorescent microorganisms.

The Kapvik microrover (Setterfield and Ellery, 2013) was available for the deployment at the Norbestos mine (Fig. 12). One of the operational goals of the deployment was to demonstrate autonomous rover navigation (path planning and path execution) and obstacle avoidance. Compared to the Pioneer rover, Kapvik provided enhanced autonomous capabilities. Given a user-specified target location, Kapvik can plan a path and navigate from its current position to this location by itself using its stereo-vision system and a scanning laser rangefinder. The instruments that were rover-mounted included a stereo three-band (Bumblebee-3) multi-spectral imager and a three-band UV–vis imager (Table 1). However, several other science instruments used in the deployment could be rover mounted because of their size (Table 1). To mitigate this issue, the non-rover mounted instruments were placed in a wheeled cart that simulated as closely as possible how such instruments would be arranged on a rover. Once the rover has completed its operations at a particular target,

Fig. 12. Kapvik rover at the Norbestos mine site.

Fig. 13. Targets visited as part of scenario 3 of the Norbestos deployment. The field of view is approximately 8 m across. The locations of the targets has been chosen to test different soil thickness (ranging from outcropping rock to a few centimeters of sand and gravel).

the instrument cart was brought to the site and measurements of the target of interest were conducted.

4.2. Operations

The operational scenarios for the rover deployment included (one day in the field was dedicated to each scenario; scenarios were progressively more complex):

- Scenario 1: visit to three pre-designated target sites. This scenario assumed that some prior scouting had been accomplished and that the Kapvik rover had been provided with three target points to visit for close-up inspection. The target points involved emplaced enhanced methane sources of different isotopic compositions in order to assess the performance of the methane characterization instrument.
- Scenario 2: visit to two targets doped with methane (and protected from dissipation by the wind). The two targets were preselected from the panoramic images of the previous day. Because the exploration zone was devoid of strong natural methane sources, they needed to be doped. The rover would navigate autonomously in the environment to visit the targets for close-up inspections. This would test the ability of both the imagery and the science team to identify high-value targets.
- Scenario 3: visit to five targets sites selected by the science team at the operations center (Fig. 13). The potential targets would be color-coded. After capturing images by Kapvik, the off-site science team would choose one of the preselected potential targets and communicate its color code to the control room (mission manager). The rover would navigate autonomously toward the selected target for close-up investigations.

High-value targets were identified using a series of sequential criteria. Initial target identification was based on visual examination of the color imagery. The images were searched specifically for the presence of surface expressions of fractures which could provide a conduit for the release of subsurface methane. Target downselection was then based on the size of the fractures, with wider fractures expected to represent deeper access to the subsurface, and the presence of tonal differences in the color imagery which could be indicative of alteration by either gas or water seepage at the surface at some time.

4.3. Discussion

Here we briefly discuss the performance of each instrument in achieving the project's science objectives.

A three-color stereocamera (Bumblebee 3) was used to facilitate autonomous navigation and target selection. It performed well, providing sufficient data for autonomous navigation as well as target selection. Target selection was based on both textural (presence of surface fissures) and color information (color differences in the imagery).

Fig. 14 shows a typical color image used for target selection, navigation and rover positioning. It was found that

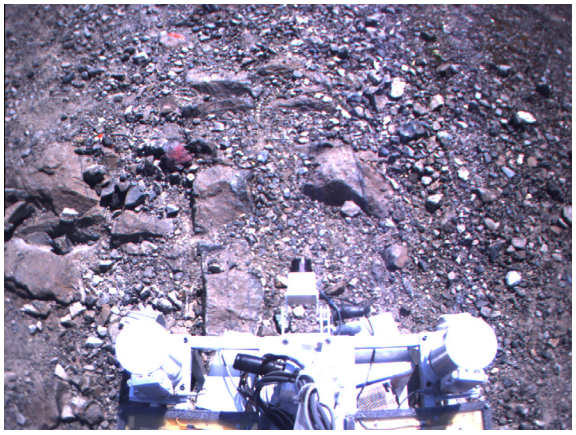

Fig. 14. Three-color image of the target area at Norbestos mine.

color fidelity was important for target selection and that the resolution of the instrument (1280 × 960 pixels) was sufficient to identify targets of interest within the test area.

Given that the Picarro instrument could not be rover mounted, gas samples were acquired at the various target points and brought to the instrument for analysis of methane concentrations and, if methane concentrations were high enough (≈25 ppm), for methane 13C/12C determinations. The Picarro methane analyzer is based on a cavity ring-down spectroscopy principle, a time-based measurement approach that uses a laser to quantify spectral features of gas phase molecules in a small optical cavity, which has an effective laser path length of up to 20 km. This allows a peak quantification of the absorption features for $_{12}CH_4$ and $_{13}CH_4$. An example of typical instrument output is shown in Fig. 15. The gas samples were introduced in the instrument and a time average was selected by the instrument operator as the value for average methane concentration at each site. This was necessitated by the fact that methane concentrations could vary over the course of an analysis.

The ASD spectrometer was used to interrogate points on rocks or soils at each target locations at Norbestos. Fig. 16 shows an example reflectance spectrum of a target acquired by this instrument. The spectrum is characterized by a number of absorption features characteristic of the target geology:

- Absorption band near 430 nm is attributable to tetrahedrally-coordinated ferric iron in serpentine (Greenberger et al., 2012).
- Absorption band near 700 nm is due to ferric–ferrous iron charge transfers.
- Narrow absorption band near 1390 nm is characteristic of hydroxyl (OH) in serpentine.
- The absorption band near 1900–2000 nm is due to water in various phases.
- The absorption band near 2320 nm is characteristic of Mg-OH combination bands in serpentine.

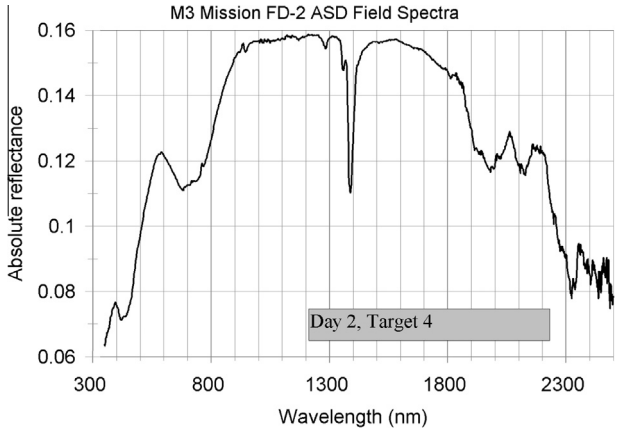

Fig. 16. A "typical" reflectance spectrum acquired in the field at the Norbestos site. Absorption features in the spectrum allow for the identification of a number of mineral components, as follows: Fe3+–Fe2+-bearing serpentine: absorption features near 430 and 700–750 nm; serpentine: narrow absorption bands near 1400 and 2320 nm; unspecified water-bearing minerals: absorption feature in the 1900–2000 nm region; unspecified metal-OH bearing phyllosilicates: absorption band in 2100 nm region.

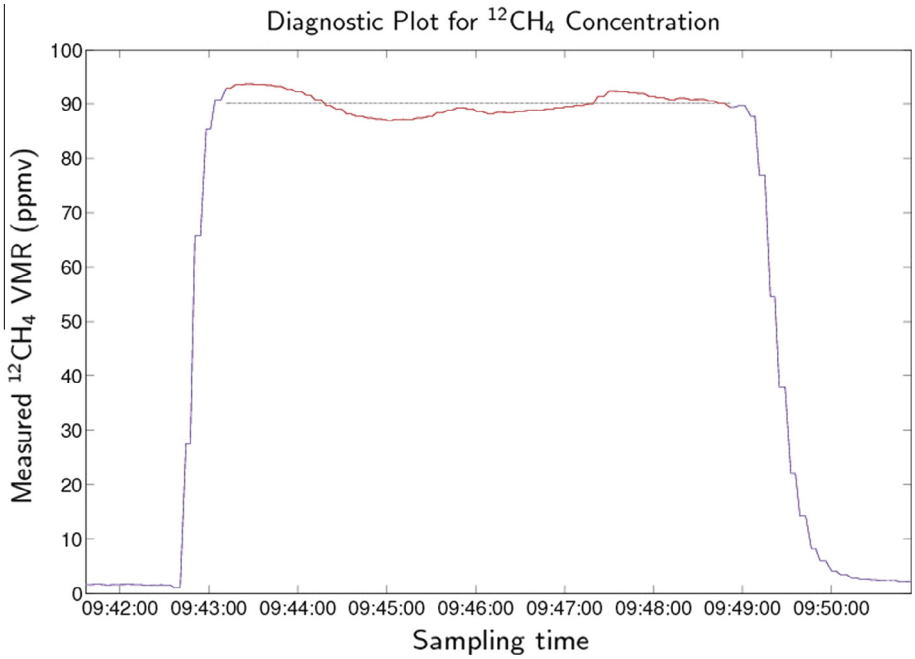

Fig. 15. Typical output spectrum of the methane concentrations as measured by the Picarro instrument at the Norbestos site. VMR: Volume Mixing Ratio.

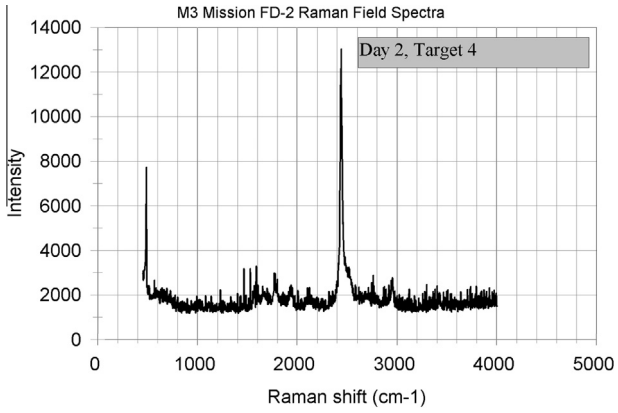

Fig. 17. A "typical" Raman spectrum acquired in the field at the Norbestos site. Raman peaks can be assigned as follows: magnetite: 450 cm^{-1} peak and ~700 and 1400 cm^{-1} humps; serpentine: ~600–700 cm^{-1} hump; magnesite: 1400–1600 cm^{-1} peaks. The nature of the 2430 cm^{-1} peak is uncertain.

Fig. 18. UV band image of the ground surface from three-band UV–vis imager acquired at the Norbestos site. The field of view is approximately 40 cm across.

It can also be seen that there are various small and narrow absorption features at various points in the spectrum that are attributable to incomplete correction of atmospheric features.

A field-portable Raman point spectrometer was also deployed. It was found that data quality varied widely from sample to sample. We attribute this to the effects of any opaque phases that may be present in the sample, fluorescence due to Fe-bearing phases, and grain size and surface texture. Nevertheless Raman spectra were successfully acquired for most of the targets (Fig. 17).

For targets exhibiting elevated methane levels, UV-induced fluorescence was deployed to determine whether these levels could be related to biological activity, in particular subsurface microorganisms residing in fissures. The instrument was deployed by shielding the target from ambient sunlight in order to observe low levels of induced fluorescence. Previous and post-deployment trials demonstrated that this system was capable of detecting even low levels of fluorescence. However, no fluorescence was detectable in the field, likely due to too-low levels of UV-fluorescing microorganisms.

In addition to the three-color stereocamera, we tested a three band imager with one of the bands located in the ultraviolet. The acquired imagery, particularly in the UV band appears to be very sensitive to viewing geometry effects (Fig. 18). In future missions, it could be used to map in-situ ilmenite based on the 320 nm/550 nm reflectance ratio, since ilmenite has a stronger reflectance in the UV than in the visible.

A hyperspectral imager from Channel System Inc., spanning the range from 400 to 700 nm was tested at the field site, as well as in the laboratory on rocks collected at the site. Preliminary analysis (Greenberger et al., 2012) shows that this wavelength region is capable of providing information on mineralogy on the basis of minor absorption bands in this region.

An electromagnetic induction sounder, loaned to the project by the Canadian Space Agency, was deployed at the Norbestos site and was used to measure changes in electrical conductivity and magnetic susceptibility across the mine site (Ralchenko et al., 2013). In the exploration zone (Fig. 10), the electrical conductivity and magnetic susceptibility were almost constant at 10 mS/m and 40 ppt, respectively. At the scale of the mine site, however, changes in these parameters could be correlated with mapped structural and petrologic features, such as the location of major shear zones, giving a "regional context" to the detailed observations made by the rover instruments.

In addition to the above instrument performance assessment, the Norbestos deployment provided a number of valuable lessons for future deployments (Cloutis et al. (2012):

- Color imagery provides a very useful baseline of data for assessing trafficability and target identification. The imagery was useful for identifying targets of interest on the basis of both tone and texture.
- For this analogue mission, a search strategy of "follow the methane" was not profitable, as methane point sources show rapid radial decreases in concentration. Concentration decay to background levels within 1 m. Even in windy environments, methane plumes do not significantly disperse in radial directions.
- Electromagnetic sounding is a useful adjunct to rover-based exploration.
- Reflectance spectra are less susceptible than Raman spectra to target physical properties.

5. Conclusions

The operations of the Mars methane analogue mission to simulate searching for methane on Mars was carried

out at the Jeffery mine in 2011 and the Norbestos mine in 2012; both are located in or near the town of Asbestos, Quebec, Canada. The sites were chosen because of their geological similarity to putative methane-producing regions on Mars. The operations were conducted over four days (Jeffrey) and five (Norbestos) days.

In the Jeffrey mine deployment, a modified off-the-shelf rover (Pioneer rover) with a vision camera and RF control was used. The rover traversed different paths with different lengths and different distances between sample points from one path to another; the distance between sample points was the same within a path. Science measurements were conducted at the traverse points where the rover stopped to acquire images and scout. Scientific sensors included Raman, Picarro, ASD, and EMIS.

In the Norbestos mine deployment, the Kapvik microrover with a stereo vision camera and RF control was used. Different strategies were used to identify targets of interest and the rover used autonomous navigation for path planning and obstacle avoidance. Science measurements were conducted at the traverse points in the context of a decision tree. Scientific sensors included Raman, Picarro, ASD, EMIS, UV-induced fluorescence, UV–vis imaging, and hyperspectral imaging.

Overall, the deployments suggested that a search strategy of "follow the methane" is not practical given the mechanisms of methane dispersion. Rather, target identification based on image tone/color and texture from panoramic imagery and in the context of identifying features that may be indicative of methane sources is more profitable.

References

Adept Mobilerobots, Pioneer 3-at data sheet, 2007.

Barnes, I., O'Neil, J.R., Trescases, J.J., 1978. Present day serpentinization in New Caledonia, Oman and Yugoslavia. Geochim. Cosmochim. Acta 42, 114–145.

Boivin, A., Samson, C., Vrionis, H., Qadi, A., Scott, C., Stromberg, J., Cloutis, E., Berard, G., Mann, P., 2011. Site selection for mars methane analogue mission: geological, astrobiological, and robotic criteria. In: Lunar Planet. Sci. Conf., 42: abstract #1472.

Boivin, A., Samson, C., Holladay, J.S., Cloutis, E., Ernst, R.E., 2012. Site selection for mars methane analogue mission (M3): near-surface electromagnetic techniques and analysis. In: Lunar Planet. Sci. Conf., 43: abstract #2140.

Boivin, A., Lai, P., Samson, C., Cloutis, E., Holladay, S., Monteiro Santos, F.A., 2013. Electromagnetic induction sounding and 3D laser imaging in support of a Mars methane analogue mission. Planet. Space Sci. 82–83, 27–33.

Burns, R.G., 1993. Mineralogical Applications of Crystal Field Theory, 2nd ed. Cambridge University Press, UK.

Clark, R.N., King, T.V.V., Klewja, M., Swayze, G.A., Vergo, N., 1990. High spectral resolution reflectance spectroscopy of minerals. J. Geophys. Res. 95 (B8), 12653–12680.

Cloutis, E.A., Vrionis, H., Qadi, A., Bell, III., J.F., Berard, G., Boivin, A., Ellery, A., Jamroz, W., Kruzelecky, R., Mann, P., Samson, C., Stromberg, J., Strong, K., Tremblay, A., Whyte, L., Wing, B., 2011a. Mars methane analogue mission (M3): analytical techniques and operations. In: Lunar Planet. Sci. Conf., 42: abstract #1174.

Cloutis, E.A., Vrionis, H., Whyte, L., Samson, C., Tremblay, A., Wing, B., Strong, K., Ellery, A., Kruzelecky, R., Bell, III., J.F., Boivin, A., Stromberg, J., Mann, P., Berard, G., 2011b. Jeffrey mine, Asbestos, Quebec, Canada: analogue site for a Mars methane mission. In: Lunar Planet. Sci. Conf., 42: abstract #6010.

Cloutis, E., Whyte, L., Qadi, A., Bell, III., J.F., Berard, G., Boivin, A., Ellery, A., Haddad, E., Jamroz, W., Kruzelecky, T., Mann, P., Olsen, K., Perrot, M., Popa, D., Rhind, T., Samson, C., Sharma, R., Stromberg, J., Strong, K., Tremblay, A., Wilhelm, R., Wing, B., Wong, B., 2012. The mars methane analogue mission (M3): results of the 2011 field deployment. In: Planet. Sci. Conf., 43: abstract #1569.

Cloutis, E., Whyte, L., Qadi, A., Anderson-Trocme, L., Bell, III., J.F., Berard, G., Boivin, A., Ellery, A., Greenberger, R., Haddad, E., Jamroz, W., Kruzelecky, T., Mann, P., Mustard, J., Olsen, K., Perrot, M., Popa, D., Ralchenko, M., Rhind, T., Samson, C., Sharma, R., Stromberg, J., Strong, K., Tremblay, A., Wing, B., 2013. The mars methane analogue mission (M3): results of the 2012 field deployment. In: Planet. Sci. Conf., 44: abstract #1579.

Ehlmann, B.L., Mustard, J.F., Murchie, S.L., et al., 2008. Orbital identification of carbonate-bearing rocks on mars. Science 322, 1828–1832.

Etiope, G., Sherwood Lollar, B., 2013. Abiotic methane on Earth. Rev. Geophys. 51, 276–299.

Etiope, G., Schoell, M., 2014. Abiotic gas: atypical but not rare. Elements 10, 291–296.

Etiope, G., Ehlmann, B.L., Schoell, M., 2013. Low temperature production and exhalation of methane from serpentinized rocks on Earth: a potential analog for methane production on Mars. Icarus 224, 276–285.

Formisano, V., Atreya, S., Encrenaz, T., et al., 2004. Detection of methane in the atmosphere of mars. Science 306, 1758–1761.

Greenberger, R.N., Mustard, J.F., Cloutis, E.A., Mann, P., Turner, K., 2012. Field hyperspectral visible imaging spectroscopy of serpentine deposits in Quebec: implications for the value of visible spectroscopy in planetary exploration. In: Geological Society of America Annual Meeting, Paper 38-5.

Hebert, R., Laurent, R., 1989. Mineral chemistry of ultramafic and mafic plutonic rocks of the appalachian ophiolites. Chem. Geol. 77, 265–285.

Klein, F., Bach, W., 2009. Fe–Ni–Co–O–S phase relations in peridotite-seawater interactions. J. Petrol. 50, 37–59.

Krasnopolsky, V.A., Maillard, J.P., Owen, T.C., 2004. First detection of methane in the martian atmosphere: evidence for life? Icarus 172, 537–547.

Lang, S.Q., Früh-Green, G.L., Bernasconi, S.M., Lilley, M.D., Proskurowski, G., Méhay, S., Butterfield, D.A., 2012. Microbial utilization of abiogenic carbon and hydrogen in a serpentinite-hosted synthesis. Geochim. Cosmochim. Acta 92, 82–99.

McCollom, T.M., Seewald, J.S., 2001. A reassessment of the potential for reduction of dissolved CO_2 to hydrocarbons during serpentinization of olivine. Geochim. Cosmochim. Acta 65, 3769–3887.

MEPAG Goals Committee, 2010. Mars science goals, objectives, and priorities. Technical report, <http://mepag.jpl.nasa.gov/reports/MEPAG_Goals_Document_2010_v17.pdf>.

Mumma, M.J., Novak, R.E., DiSanti, M.A., Bonev, B.P., 2003. A sensitive search for methane on Mars. Am. Astron. Soc. Bull. 35, 937–938.

Mumma, M.J., Villanueva, G.L., Novak, R.E., et al., 2009. Strong release of methane on mars in northern summer 2003. Science 323, 1041–1045.

Normand, C., Williams-Jones, A.E., 2007. Physiochemical conditions and timing of rodingite formation: evidence from rodingite-hosted fluid inclusions in the JM asbestos mine. Geochem. Trans. 8, 11–30.

Olsen, K.S., Cloutis, E., Strong, K., 2012. Small-scale methane dispersion modelling for possible plume sources on the surface of mars. Geophys. Res. Lett. 39, L19201.

Ralchenko, M., Perrot, M., Samson, C., Tremblay, A., Holladay, S., Cloutis, E., 2013. Mars Methane Analogue Mission (M3): Geological

mapping with an electromagnetic induction sounder. In: Lunar Planet. Sci. Conf., 44: abstract #1027.

Schroetter, J.-M., Bedard, H., Tremblay, A., 2005. Structural evolution of the thetford mines ophiolite complex, Canada: implications for the southern Quebec ophiolitic belt. Tectonics 24 (TC1001).

Schulte, M., Blake, D., Hoehler, T., McCollom, T., 2006. Serpentinization and its implications for life on the Early Earth and Mars. Astrobiology 6, 364–376.

Setterfield, T.P., Ellery, A., 2013. Terrain response estimation using an instrumental rocker-bogie mobility system. IEEE Trans. Rob. 29 (1), 172–188.

Tremblay, A., Castonguay, S., 2002. Structural evolution of the laurentian margin revisited (southern quebec appalachians): implications for the salinian orogeny and successor basins. Geology 30, 79–82.

Zahnle, K., Freedman, R.S., Catling, D.C., 2011. Is there methane on Mars? Icarus 212, 493–503.